

Localized Particle States and Dynamic Gravitational Effects

Ian H. Redmount*

Department of Physics

Parks College of Engineering, Aviation, and Technology

Saint Louis University

St. Louis, Missouri 63103-1110 USA

(Dated: March 11, 2018)

Scalar particles—i.e., scalar-field excitations—in de Sitter space exhibit behavior unlike either classical particles in expanding space or quantum particles in flat spacetime. Their energies oscillate forever, and their interactions are spread out in energy. Here it is shown that these features characterize not only normal-mode excitations spread out over all space, but localized particles or wave packets as well. Both one-particle and coherent states of a massive, minimally coupled scalar field in de Sitter space, associated with classical wave packets, are constructed explicitly. Their energy expectation values and corresponding Unruh-DeWitt detector response functions are calculated. Numerical evaluation of these quantities for a simple set of classical wave packets clearly displays these novel features. Hence, given the observed accelerating expansion of the Universe, it is possible that observation of an ultralow-mass scalar particle could yield direct confirmation of distinct predictions of quantum field theory in curved spacetime.

PACS numbers: 04.62.+v

Keywords: quantized fields, de Sitter space, scalar particles

I. INTRODUCTION

Although quantum field theory in curved spacetime is widely regarded as a mature, even a finished field, experimental or observational confirmations of its predictions are lacking. It is therefore of interest to seek phenomena within the theory—entailing both field quantization and nontrivial spacetime geometry—which might come within reach of actual measurement. Effects of quantized fields on the evolution of spacetime, e.g., via black-hole evaporation [1] or cosmological inflation [2], have been extensively studied for decades, but direct observation of either phenomenon has proved elusive. It is possible to look in the other direction: for effects of spacetime geometry—in particular, of spacetime *dynamics*—on quantized-field excitations, i.e., on the measurable properties of elementary particles. The possibility that precise measurements of particle properties might probe the dynamics of the cosmos is an intriguing one.

In 1989 I described the behavior of scalar particles, i.e., excitations of a real, linear, scalar field, in de Sitter space [3]. Modulation of the field normal modes by the vigorous dynamics of that spacetime causes those excitations to behave unlike either classical particles in an expanding universe or quantized-field excitations in a static spacetime: Their energy expectation values, above that of the vacuum, oscillate at late and early times with fixed amplitude and frequency, rather than redshifting to a constant value (the field mass). And their interactions with a “detector” coupled to the field, again above the vacuum value, describe not a finite transition *rate*

at fixed energy but a finite transition *probability* over all time, with finite width in energy. That is, the detector fails to fix the energy of an excitation at a specific value. This effect is also found for scalar-field excitations in a suitably dynamic “laboratory” setting in flat spacetime [4].

At the time, however, these phenomena might have been regarded as arcane curiosities, for several reasons: The expansion of an ordinary matter- or radiation-dominated universe is far less vigorous than the hyperbolic or exponential expansion of de Sitter space, suppressing the effects. And these effects are apparent only for excitations of a field with Compton wavelength comparable to the curvature radius of the spacetime, being strongly suppressed for larger masses. In the early universe this might encompass fields with GUT-scale masses, but that epoch is inaccessible to direct observation; in the present era this would require a mass far smaller than that of any known particle. (Conformally invariant *massless* fields, such as that of the photon, do not exhibit such effects at all.) Also, the normal modes of the field correspond to field configurations extending over all space; observed particles are associated with localized wave packets.

Recent discoveries, however, have vitiated some of these objections. Detailed observations of Type Ia supernova distributions [5] and of the cosmic microwave background suggest that the present Universe is dominated not by matter or radiation but by cosmological-constant, vacuum, or “dark energy” contributions, making de Sitter expansion a better approximation to cosmological dynamics than previously apparent. Moreover, Parker and Raval [6, 7] have shown that the vacuum-energy effects of a linear scalar field with mass of order 10^{-33} eV can account quite tidily for the observed expansion of the Universe. Such a mass corresponds to a Compton wavelength

*Electronic address: redmouih@slu.edu

of order 10^{26} m, the same order as the curvature radius of a de Sitter-like spacetime with Hubble parameter, say, 75 km/s/Mpc. If the particles (excitations) of Parker's and Raval's proposed field can be detected, they might exhibit the dynamical effects I have described. Burko, Harte, and Poisson [8] have also shown that a *classical* scalar particle in an expanding universe can display unusual behavior—a nonconstant mass—with potentially observable consequences.

In this work I show that the novel dynamical features of normal-mode excitations of a scalar field in de Sitter space can persist in field states describing localized wave packets, e.g., first-quantized or classical particles. I construct several classes of (second-quantized) field states associated with classical solutions of the field equation. I then obtain exact expressions for excitation energies and monopole-detector response functions in these states. Numerical evaluation of these results for a simple choice of wave packet illustrates the effects sought, and suggests further avenues of exploration.

The spacetime geometry and field theory used here are described in Sec. II below. Quantum states suitable for describing localized field configurations are given explicitly in Sec. III, and their energies and detector responses are calculated. Numerical results for sample wave packets are shown in Sec. IV. The results and their implications are summarized in Sec. V. Throughout I use units giving $\hbar = c = 1$; sign conventions and general notation follow those of Ref. 9.

II. SPACETIME AND FIELD

A. de Sitter-space geometry

de Sitter space provides a suitably dynamic background geometry. This spacetime can be given coordinates with closed (spherical), flat, or open (hyperbolic) spatial sections. Although recent evidence suggests the latter two may be more appropriate to the actual Universe [5, 10], I use the first here for simplicity. For $N + 1$ -dimensional de Sitter space (a straightforward generalization of $3 + 1$ dimensions), convenient coordinates are comoving-observer proper time $t \in (-\infty, +\infty)$, $N - 1$ polar angles $\theta_1, \dots, \theta_{N-1} \in [0, \pi]$, and one azimuthal angle $\phi \in [0, 2\pi)$. The spacetime metric takes the form

$$ds^2 = -dt^2 + a^2 \cosh^2(t/a) d\Omega_N^2 \quad (2.1)$$

in these coordinates, where a is a positive constant and $d\Omega_N^2$ the metric of the unit N -sphere.

B. Scalar field theory

A real, linear, massive, minimally coupled, quantized scalar field serves as a simple example. The field φ , with mass μ , has Lagrangian density

$$\mathcal{L} = -\frac{1}{2}(\nabla_\alpha \varphi \nabla^\alpha \varphi + \mu^2 \varphi^2) \quad (2.2)$$

and corresponding field equation

$$(\square - \mu^2) \varphi = 0, \quad (2.3)$$

where \square is the covariant d'Alembertian in $N + 1$ -dimensional de Sitter space.

Quantized fields in de Sitter space have been studied extensively since the 1950's [11]. A thorough description of the approach used here, with references to some of the enormous literature, is given in Ref. 3. In this section I briefly summarize the features of this model appropriate to the present problem.

1. Canonical quantization

Canonical quantization of this field is effected via an expansion of φ in normal modes, with operator coefficients, thus:

$$\varphi(t, \Omega_N) = a^{-N/2} \sum_L [b_L \chi_L(t) + b_L^\dagger \chi_L^*(t)] \mathcal{Y}_L(\Omega_N). \quad (2.4)$$

Here Ω_N denotes the angular coordinates $\theta_1, \dots, \theta_{N-1}, \phi$ collectively, and L denotes the set of angular-momentum quantum numbers identifying the normal modes. The N -dimensional spherical harmonics \mathcal{Y}_L can be given explicitly as

$$\begin{aligned} \mathcal{Y}_L(\Omega_N) = & \prod_{j=1}^{N-1} \left[\left(\lambda_j \frac{(\lambda_j - \frac{1}{2} + \lambda_{j+1})!}{(\lambda_j - \frac{1}{2} - \lambda_{j+1})!} \right)^{1/2} \right. \\ & \times (\sin \theta_j)^{(j+1-N)/2} P_{\lambda_j - (1/2)}^{-\lambda_{j+1}}(\cos \theta_j) \left. \right] \\ & \times [\pi(1 + \delta_{l_N 0})]^{-1/2} \begin{Bmatrix} \cos(l_N \phi) \\ \sin(l_N \phi) \end{Bmatrix}, \end{aligned} \quad (2.5a)$$

with

$$\lambda_j \equiv l_j + \frac{N-j}{2} \quad (2.5b)$$

and

$$l_1 \geq l_2 \geq \dots \geq l_{N-1} \geq l_N \geq 0 \quad (2.5c)$$

the integer quantum numbers making up the set L . Here the P 's are associated Legendre functions of the first kind, and the harmonics are chosen real for convenience. The time-dependence functions χ_L can be written

$$\begin{aligned} \chi_L(t) = & \left(\frac{a\pi/2}{\sinh(\pi qa)} \right)^{1/2} \cosh^{-N/2}(t/a) \\ & \times \left\{ \kappa_L^{(+)} P_{\lambda_1 - 1/2}^{-iqa}[\tanh(t/a)] + \kappa_L^{(-)} P_{\lambda_1 - 1/2}^{+iqa}[\tanh(t/a)] \right\}, \end{aligned} \quad (2.6a)$$

with parameter

$$q \equiv \left(\mu^2 - \frac{N^2}{4a^2} \right)^{1/2} \quad (2.6b)$$

and constants $\kappa_L^{(\pm)}$ satisfying $|\kappa_L^{(+)}|^2 - |\kappa_L^{(-)}|^2 = 1$. The form and behavior of the functions differ for real and imaginary values of q . Here I shall take q real, i.e., mass satisfying $\mu > N/(2a)$.

The operator coefficients b_L and b_L^\dagger in expansion (2.4) play the usual role of field-excitation annihilation and creation operators, respectively. They satisfy commutation relations $[b_L, b_{L'}^\dagger] = \delta_{LL'}$, *et cetera*.

2. Functional Schrödinger description

Quantum states of the field φ can also be described by wave functionals $\Psi[\varphi(\Omega_N), t]$, which depend on the configuration of the field on constant-time hypersurfaces of the de Sitter geometry, and the time. The wave functionals are solutions of a functional Schrödinger equation [12, 13]

$$i \frac{\partial}{\partial t} \Psi = H \Psi, \quad (2.7a)$$

with Hamiltonian operator

$$H = \int d\Omega_N a^N \cosh^N(t/a) |g_{tt}|^{-1/2} T_{tt} \quad (2.7b)$$

constructed from the spacetime metric and the canonical stress-energy tensor

$$T_{\alpha\beta} = \nabla_\alpha \varphi \nabla_\beta \varphi + g_{\alpha\beta} \mathcal{L} \quad (2.7c)$$

of the field, where \mathcal{L} is the Lagrangian density (2.2). (For the minimally coupled field φ , this tensor coincides with the gravitational stress-energy tensor obtained by variation of the field action with respect to the metric.) The Hamiltonian is rendered a functional differential operator via the representation of the field momentum

$$\Pi = \nabla_t \varphi \rightarrow i g_{tt} |g|^{-1/2} \frac{\delta}{\delta \varphi}, \quad (2.8)$$

with g the metric determinant, paralleling the representation of momentum in ordinary quantum mechanics.

The Hamiltonian takes a particularly simple form in terms of the amplitudes with which the field configuration is expanded in spherical harmonics. With expansion

$$\varphi(\Omega_N) = a^{(1-N)/2} \sum_L y_L \mathcal{Y}_L(\Omega_N) \quad (2.9)$$

—an expansion of the field on a single constant-time hypersurface, not on the entire spacetime as in Eq. (2.4)—the Hamiltonian becomes

$$H = \sum_L \left(-\frac{\text{sech}^N(t/a)}{2a} \frac{\delta^2}{\delta y_L^2} + \frac{a \cosh^N(t/a)}{2} \omega_L^2 y_L^2 \right), \quad (2.10a)$$

a sum of independent “harmonic oscillator” Hamiltonians with time-dependent “angular frequencies”

$$\omega_L = \left(\mu^2 + \frac{\ell_1(\ell_1 + N - 1)}{a^2 \cosh^2(t/a)} \right)^{1/2}. \quad (2.10b)$$

The Hamiltonian can also be expressed in terms of the amplitude operators and time-dependence functions of expansion (2.4). It then becomes

$$H = \frac{\cosh^N(t/a)}{2} \sum_L \left[(b_L^\dagger b_L + b_L b_L^\dagger) (\dot{\chi}_L \dot{\chi}_L^* + \omega_L^2 \chi_L \chi_L^*) + b_L^2 (\dot{\chi}_L^2 + \omega_L^2 \chi_L^2) + b_L^{\dagger 2} (\dot{\chi}_L^{*2} + \omega_L^2 \chi_L^{*2}) \right], \quad (2.11)$$

where overdots denote time derivatives. The annihilation operators are represented in the functional Schrödinger description as

$$b_L = -ia^{1/2} \cosh^N(t/a) \dot{\chi}_L^* y_L + a^{-1/2} \chi_L^* \frac{\delta}{\delta y_L}, \quad (2.12)$$

with the creation operators b_L^\dagger the Hermitian conjugate of this.

3. Excitation-number eigenstates

A Fock space of quantum states for the field φ is spanned by eigenstates of the excitation-number operators $b_L^\dagger b_L$. These have wave functionals

$$\begin{aligned} \Psi_{\{n_L\}}[\{y_L\}, t] &= \prod_L \left(\frac{a}{2\pi} \right)^{1/4} (2^{n_L} n_L!)^{-1/2} \\ &\times [\chi_L^*(t)]^{-1/2} \left(\frac{\chi_L(t)}{\chi_L^*(t)} \right)^{n_L/2} H_{n_L}[\Delta_L^{1/2}(t) y_L] \\ &\times \exp\left\{ -\frac{1}{2} [\Delta_L(t) - i\bar{\Delta}_L(t)] y_L^2 \right\} \end{aligned} \quad (2.13a)$$

with

$$\Delta_L(t) = \frac{a}{2|\chi_L(t)|^2}, \quad (2.13b)$$

$$\bar{\Delta}_L(t) = \frac{a \cosh^N(t/a)}{2|\chi_L(t)|^2} \frac{d}{dt} |\chi_L(t)|^2, \quad (2.13c)$$

and each H_{n_L} an Hermite polynomial of order n_L . The nonnegative integral excitation numbers n_L for all the normal modes of the field are exact constants of the states’ evolution; the set $\{n_L\}$ identifies each eigenstate. These are not, however, eigenstates of the Hamiltonian (2.10a) or (2.11). These states form an orthonormal basis:

$$\begin{aligned} \langle \{n_L\} | \{n'_L\} \rangle &= \int \Psi_{\{n_L\}}^*[\{y_L\}, t] \Psi_{\{n'_L\}}[\{y_L\}, t] \prod_L dy_L \\ &= \prod_L \delta_{n_L n'_L} \end{aligned} \quad (2.14)$$

in bra-and-ket notation.

The expectation value of the field φ in any of these eigenstates is zero. Each wave functional (2.13a) is of definite parity in each field amplitude y_L , implying

$$\begin{aligned} \langle \{n_L\} | \varphi | \{n_L\} \rangle (t, \Omega_N) &= \int \Psi_{\{n_L\}}^* [\{y_L\}, t] \\ &\times \left(a^{(1-N)/2} \sum_L y_L \mathcal{Y}_L(\Omega_N) \right) \Psi_{\{n_L\}} [\{y_L\}, t] \prod_L dy_L \\ &= 0. \end{aligned} \quad (2.15)$$

Of course the same result follows from expansion (2.4), the annihilation and creation properties of the amplitude operators, and the orthonormality relation (2.14).

The expectation value of the field energy—as defined by Hamiltonian (2.10a) or (2.11)—in an excitation-number eigenstate consists of a “vacuum energy,” plus a sum of excitation energies for each mode times the number of excitations in that mode. This can be written

$$\langle \{n_L\} | H | \{n_L\} \rangle (t) = \langle \{0\} | H | \{0\} \rangle + \sum_L n_L E_L(t), \quad (2.16a)$$

with

$$E_L(t) = \frac{a^2 \omega_L^2 \cosh^{2N}(t/a) + \Delta_L^2 + \bar{\Delta}_L^2}{2a \Delta_L \cosh^N(t/a)}. \quad (2.16b)$$

The vacuum contribution $\langle \{0\} | H | \{0\} \rangle$, sometimes described as a “particle content,” has been extensively analyzed [14, 15, 16]. It is the energy E_L , however, which is associated with a “particle” in the sense of an excitation of the field. For a minimally coupled field (specifically, for any except a massless, conformally coupled field), E_L behaves quite unlike a classical energy. For mass $\mu > N/(2a)$ as assumed here, it oscillates at late times $t \gg a$:

$$E_L(t) \sim \frac{\mu^2}{q} \cosh \alpha_L + \frac{N\mu}{2qa} \sinh \alpha_L \cos(2qt - \beta_L), \quad (2.17a)$$

where the parameters α_L and β_L are determined by the constants $\kappa_L^{(\pm)}$ which fix the normal-mode time-dependence (“positive-frequency”) functions χ_L , as in Eq. (2.6a), viz.,

$$\alpha_L = 2 \operatorname{Arccosh} |\kappa_L^{(+)}| = 2 \operatorname{Arcsinh} |\kappa_L^{(-)}|, \quad (2.17b)$$

$$\beta_L = \arg \left[\kappa_L^{(+)} \kappa_L^{(-)*} \left(\frac{N}{2} + iqa \right) \right] - 2 \arg \Gamma(1 + iqa). \quad (2.17c)$$

The oscillations of the energy E_L do not damp out; their amplitude is asymptotically constant. For the minimally coupled field considered here, the oscillating E_L remain always positive.

Field states can also be characterized by the response of an Unruh-DeWitt “monopole detector” [17, 18] coupled linearly to the field. The probability of the detector making a transition of energy E —with the field in

state $|\{n_L\}\rangle$ —is proportional to a response function independent of the detector’s structure, viz.,

$$\begin{aligned} \mathcal{F}_{\{n_L\}}[E, x(\tau)] &= \int_{-\infty}^{+\infty} \int_{-\infty}^{+\infty} e^{-iE(\tau_1 - \tau_2)} \\ &\times \langle \{n_L\} | \varphi[x(\tau_1)] \varphi[x(\tau_2)] | \{n_L\} \rangle d\tau_1 d\tau_2, \end{aligned} \quad (2.18)$$

where $x(\tau)$ denotes the coordinates of the detector’s worldline at proper time τ . For a detector comoving in the geometry of metric (2.1), at angular coordinates Ω_N , this too decomposes into a vacuum contribution plus contributions from each excitation:

$$\begin{aligned} \mathcal{F}_{\{n_L\}}(E, \Omega_N) &= \mathcal{F}_{\{0\}}(E, \Omega_N) \\ &+ a^{-N} \sum_L n_L [|X_L(E)|^2 + |X_L(-E)|^2] \mathcal{Y}_L^2(\Omega_N), \end{aligned} \quad (2.19a)$$

with $X_L(E)$ the Fourier transform

$$\begin{aligned} X_L(E) &= \int_{-\infty}^{+\infty} e^{-iEt} \chi_L(t) dt \\ &= \frac{2^{(N-2)/2} a}{(2q)^{1/2} \Gamma(N/2)} \\ &\times [\kappa_L^{(+)} \Xi(+q, \lambda_1, E) + \kappa_L^{(-)} \Xi(-q, \lambda_1, E)] \end{aligned} \quad (2.19b)$$

and

$$\begin{aligned} \Xi(q, \lambda_1, E) &= \left(\frac{\Gamma(1 - iqa)}{\Gamma(1 + iqa)} \right)^{1/2} \Gamma \left(\frac{N}{4} + \frac{i(E+q)a}{2} \right) \\ &\times \Gamma \left(\frac{N}{4} - \frac{i(E+q)a}{2} \right) \\ &\times {}_3F_2 \left(\frac{1}{2} - \lambda_1, \frac{1}{2} + \lambda_1, \frac{N}{4} + \frac{i(E+q)a}{2}; 1 + iqa, \frac{N}{2}; 1 \right). \end{aligned} \quad (2.19c)$$

In Minkowski space the transform X is a delta function in energy. The response function \mathcal{F} thus contains a factor enforcing energy conservation, and a factor of the total time interval, by which it is divided to give a response rate. In de Sitter space, however, the response probability associated with an excitation is finite and has finite width in energy, reflecting the influence of the dynamic spacetime geometry.

The choice of coefficients $\kappa_L^{(\pm)}$ appearing in Eqs. (2.6a), (2.17), and (2.19b) is tantamount to the choice of vacuum state on which the state space of the field is based. Many authors have examined the variety of vacuum states available for a scalar field in de Sitter space [19]. For many reasons, the Euclidean [20] or Chernikov-Tagirov [21] vacuum emerges as the most appropriate choice [3]. The

coefficients corresponding to that choice are

$$\kappa_L^{(+)} = \frac{2^{iqa} e^{-i\pi(\lambda_1 - 1/2)/2}}{(1 - e^{-2\pi qa})^{1/2}} \times \left(\frac{\Gamma\left(\frac{\frac{3}{2} + \lambda_1 + iqa}{2}\right) \Gamma\left(\frac{\frac{1}{2} + \lambda_1 + iqa}{2}\right)}{\Gamma\left(\frac{\frac{3}{2} + \lambda_1 - iqa}{2}\right) \Gamma\left(\frac{\frac{1}{2} + \lambda_1 - iqa}{2}\right)} \right)^{1/2} \quad (2.20a)$$

$$\kappa_L^{(-)} = \frac{2^{-iqa} e^{-i\pi(\lambda_1 + 3/2)/2}}{(e^{2\pi qa} - 1)^{1/2}} \times \left(\frac{\Gamma\left(\frac{\frac{3}{2} + \lambda_1 - iqa}{2}\right) \Gamma\left(\frac{\frac{1}{2} + \lambda_1 - iqa}{2}\right)}{\Gamma\left(\frac{\frac{3}{2} + \lambda_1 + iqa}{2}\right) \Gamma\left(\frac{\frac{1}{2} + \lambda_1 + iqa}{2}\right)} \right)^{1/2} . \quad (2.20b)$$

This choice will be used here in all subsequent calculations.

III. LOCALIZED PARTICLE STATES

A. “Smearred” one-particle states

A simple way to associate an excited state of the field φ with a localized “wave packet” is to “smear” the field operator φ with a suitable classical solution Φ of the wave equation (2.3), and apply the resulting operator to the vacuum state $|\{0\}\rangle$. The result is a superposition of one-particle states:

$$|\Phi\rangle_1 = (\Phi, \varphi) |\{0\}\rangle , \quad (3.1a)$$

where the smeared field operator is the Klein-Gordon inner product

$$(\Phi, \varphi) = i \int \left(\Phi \dot{\varphi} - \dot{\Phi} \varphi \right) a^N \cosh^N(t/a) d\Omega_N . \quad (3.1b)$$

If the classical wave packet Φ is given by the expansion

$$\Phi(t, \Omega_N) = a^{-N/2} \sum_L [\xi_L \chi_L(t) + \xi_L^* \chi_L^*(t)] \mathcal{Y}_L(\Omega_N) , \quad (3.2)$$

with c -number coefficients ξ_L , then operator expansion (2.4) and the orthonormality of the normal-mode basis functions imply

$$(\Phi, \varphi) = \sum_L (\xi_L^* b_L - \xi_L b_L^\dagger) . \quad (3.3)$$

The smeared one-particle state is then

$$|\Phi\rangle_1 = - \sum_L \xi_L |1_L\rangle , \quad (3.4)$$

where the kets on the right denote excitation-number eigenstates with one excitation in the L mode and zero in all others. The state $|\Phi\rangle_1$ is normalized to unity if the normalization condition

$$\sum_L |\xi_L|^2 = 1 \quad (3.5)$$

is imposed on Φ . Because this state is a superposition of single-excitation particle-number eigenstates, the expectation value of the field φ in this state is zero, just as for a single eigenstate.

The excitation energy of this state, i.e., the expectation value of the field Hamiltonian above the vacuum value, follows from Eq. (2.16a). It is

$$\begin{aligned} \mathcal{E}_1(\{\xi_L\}, t) &= {}_1\langle \Phi | H | \Phi \rangle_1 - \langle \{0\} | H | \{0\} \rangle \\ &= \sum_L |\xi_L|^2 E_L(t) , \end{aligned} \quad (3.6)$$

with the E_L from Eq. (2.16b).

The detector response function for this state can be calculated as in Eq. (2.18). For a comoving detector, the result is

$$\begin{aligned} \mathcal{F}_\Phi^{(1)}(E, \Omega_N) &= \mathcal{F}_{\{0\}}(E, \Omega_N) \\ &\quad + |\tilde{\Phi}_+(E, \Omega_N)|^2 + |\tilde{\Phi}_+(-E, \Omega_N)|^2 , \end{aligned} \quad (3.7a)$$

where

$$\tilde{\Phi}_+(E, \Omega_N) \equiv a^{-N/2} \sum_L \xi_L X_L(E) \mathcal{Y}_L(\Omega_N) , \quad (3.7b)$$

with X_L from Eq. (2.19b), is the temporal Fourier transform of the “positive frequency” part of the wave packet Φ .

B. States with nonzero $\langle \varphi \rangle$

One feature which might be expected of a quantum-field-theoretic description of a classical or “first-quantized” particle, but which does not appear in the smeared one-particle state, is a nonzero expectation value for the wave field φ . This can be obtained via an admixture of vacuum and one-particle states. For example, the state

$$|\Phi\rangle_\epsilon = \cos \epsilon |\{0\}\rangle - \sin \epsilon |\Phi\rangle_1 \quad (3.8)$$

has field expectation value

$$\epsilon \langle \Phi | \varphi | \Phi \rangle_\epsilon = \sin \epsilon \cos \epsilon \Phi(t, \Omega_N) . \quad (3.9)$$

The energy of this state above the vacuum is

$$\mathcal{E}_\epsilon(\{\xi_L\}, t) = \sin^2 \epsilon \mathcal{E}_1(\{\xi_L\}, t) , \quad (3.10)$$

with \mathcal{E}_1 from Eq. (3.6). The detector response function for this state is

$$\begin{aligned} \mathcal{F}_\Phi^{(\epsilon)}(E, \Omega_N) &= \mathcal{F}_{\{0\}}(E, \Omega_N) \\ &\quad + \sin^2 \epsilon [|\tilde{\Phi}_+(E, \Omega_N)|^2 + |\tilde{\Phi}_+(-E, \Omega_N)|^2] , \end{aligned} \quad (3.11)$$

with $\tilde{\Phi}_+$ again from Eq. (3.7b).

C. Coherent states

Perhaps the most appropriate description of a ‘‘classical’’ particle or wave packet in quantum field theory is a coherent state or Glauber state [22], akin to those states embodying classical behavior in a quantum harmonic oscillator. These states can be constructed by applying a ‘‘displacement operator’’ [23, 24] to the field ground state:

$$|\Phi\rangle_c = \prod_L D_L(\xi_L) |\{0\}\rangle, \quad (3.12a)$$

with

$$D_L(\xi_L) \equiv \exp(\xi_L b_L^\dagger - \xi_L^* b_L). \quad (3.12b)$$

Clearly this state is a superposition of all particle-number eigenstates. It can be written

$$\begin{aligned} |\Phi\rangle_c &= \prod_L \exp(-\tfrac{1}{2}|\xi_L|^2) \exp(\xi_L b_L^\dagger) \exp(-\xi_L^* b_L) |0\rangle_L \\ &= e^{-\frac{1}{2} \sum_L |\xi_L|^2} \prod_L \left(\sum_{k=0}^{\infty} \frac{\xi_L^k}{\sqrt{k!}} |k\rangle_L \right). \end{aligned} \quad (3.13)$$

Here $|k\rangle_L$ denotes the k th excited state of the L field mode, and the normalization (3.5) is again assumed.

An explicit wave functional for this state can be obtained by using operator representation (2.12). With the time dependence of each term in expansion (3.2) of Φ ,

$$Y_L(t) \equiv a^{-1/2} [\xi_L \chi_L(t) + \xi_L^* \chi_L(t)], \quad (3.14a)$$

and a corresponding time derivative

$$\mathcal{P}_L(t) \equiv a^{1/2} \cosh^N(t/a) [\xi_L \dot{\chi}_L(t) + \xi_L^* \dot{\chi}_L(t)], \quad (3.14b)$$

the displacement operator takes the form

$$\begin{aligned} D_L(\xi_L) &= \exp\left(i\mathcal{P}_L y_L - Y_L \frac{\delta}{\delta y_L}\right) \\ &= e^{-\frac{i}{2}\mathcal{P}_L Y_L} e^{i\mathcal{P}_L y_L} e^{-Y_L \frac{\delta}{\delta y_L}}. \end{aligned} \quad (3.14c)$$

Applying these operators to a wave functional of form (2.13a) for the vacuum state yields the wave functional

$$\begin{aligned} \Psi_\Phi^{(c)}[\{y_L\}, t] &= \prod_L \left(\frac{a}{2\pi}\right)^{1/4} [\chi_L^*(t)]^{-1/2} e^{-\frac{i}{2}\mathcal{P}_L Y_L} e^{i\mathcal{P}_L y_L} \\ &\quad \times \exp\left\{-\frac{1}{2}[\Delta_L(t) - i\bar{\Delta}_L(t)](y_L - Y_L)^2\right\} \end{aligned} \quad (3.15)$$

for the coherent state corresponding to the classical field Φ .

Expectation values of operators in this state match closely the corresponding classical quantities. The expectation value of the field is

$${}_c\langle\Phi|\varphi|\Phi\rangle_c = \Phi(t, \Omega_N). \quad (3.16)$$

The excitation energy of the state, above the vacuum, is

$$\begin{aligned} \mathcal{E}_c(\{\xi_L\}, t) &= \sum_L \left(\frac{\operatorname{sech}^N(t/a)}{2a} \mathcal{P}_L^2(t) \right. \\ &\quad \left. + \frac{a \cosh^N(t/a)}{2} \omega_L^2(t) Y_L^2(t) \right). \end{aligned} \quad (3.17)$$

The operator identity

$$e^A B e^{-A} = \sum_{n=0}^{\infty} \frac{1}{n!} [A, B]^{(n)}, \quad (3.18a)$$

with

$$[A, B]^{(0)} \equiv B \quad (3.18b)$$

and

$$[A, B]^{(n)} \equiv [A, [A, B]^{(n-1)}], \quad (3.18c)$$

as may be proved by induction, implies, e.g.,

$$b_L D_L(\xi_L) = D_L(\xi_L) (b_L + \xi_L) \quad (3.19a)$$

and

$$[D_L(\xi_L)]^\dagger b_L^\dagger = (b_L^\dagger + \xi_L^*) [D_L(\xi_L)]^\dagger \quad (3.19b)$$

These can be used to evaluate the comoving-detector response function in the coherent state, yielding

$$\begin{aligned} \mathcal{F}_c(E, \Omega_N) &= \mathcal{F}_{\{0\}}(E, \Omega_N) + |\tilde{\Phi}(E, \Omega_N)|^2 \\ &= \mathcal{F}_{\{0\}}(E, \Omega_N) \\ &\quad + [\tilde{\Phi}_+(E, \Omega_N) + \tilde{\Phi}_+^*(-E, \Omega_N)] \\ &\quad \times [\tilde{\Phi}_+(-E, \Omega_N) + \tilde{\Phi}_+^*(E, \Omega_N)] \\ &= \mathcal{F}_\Phi^{(1)}(E, \Omega_N) \\ &\quad + 2\Re[\tilde{\Phi}_+(E, \Omega_N)\tilde{\Phi}_+(-E, \Omega_N)], \end{aligned} \quad (3.20a)$$

with

$$\tilde{\Phi}(E, \Omega_N) \equiv \int_{-\infty}^{\infty} e^{-iEt} \Phi(t, \Omega_N) dt \quad (3.20b)$$

the temporal Fourier transform of the *full* wave packet Φ , and $\mathcal{F}_\Phi^{(1)}$ and $\tilde{\Phi}_+(E, \Omega_N)$ from Eqs. (3.7). Result (3.20a) shows that as long as $\Re[\tilde{\Phi}_+(E, \Omega_N)\tilde{\Phi}_+(-E, \Omega_N)]$ is nonzero, an Unruh-DeWitt detector can distinguish between the smeared one-particle state and the coherent field state for the same classical field configuration Φ .

IV. EXAMPLE: A GAUSSIAN WAVE PACKET

To illustrate the persistence of spacetime-dynamical effects on a localized particle, I use a simple—if somewhat

unrealistic—classical wave packet: a momentarily static, spherically symmetric Gaussian field at the instant of minimal spatial radius ($t = 0$), centered on the "north pole" ($\theta_1 = 0$) of the de Sitter space. This is specified via

$$\Phi(0, \Omega_N) = \frac{K}{(2\pi\sigma^2)^{1/2}} \exp\left(-\frac{\theta_1^2}{2\sigma^2}\right) \quad (4.1a)$$

and

$$\dot{\Phi}(0, \Omega_N) = 0, \quad (4.1b)$$

where constant σ represents the width of the initial Gaussian and K is determined numerically by enforcing condition (3.5). A separate normalization of the form $[a \cosh(t/a)]^N \int \Phi^2 d\Omega_N$ is not imposed, as the field equation (2.3) does not preserve such a condition.

For numerical calculations, it is convenient to write the time-dependence functions (2.6a) in the equivalent form

$$\chi_L(t) = \left(\frac{a}{2\Re\gamma_L}\right)^{1/2} \left(f_1(t) - i\frac{\gamma_L}{a}f_2(t)\right), \quad (4.2a)$$

with

$$f_1(t) = [\cosh(t/a)]^{-N/2-iqua} \times F\left(\frac{\frac{1}{2} + \lambda_1 + iqa}{2}, \frac{\frac{1}{2} - \lambda_1 + iqa}{2}; \frac{1}{2}; \tanh^2(t/a)\right) \quad (4.2b)$$

and

$$f_2(t) = [\cosh(t/a)]^{-N/2-iqua} \times F\left(\frac{\frac{3}{2} + \lambda_1 + iqa}{2}, \frac{\frac{3}{2} - \lambda_1 + iqa}{2}; \frac{3}{2}; \tanh^2(t/a)\right), \quad (4.2c)$$

the F 's here denoting ordinary hypergeometric functions. The parameters

$$\gamma_L = \Delta_L(0) - i\bar{\Delta}_L(0) = ia\frac{\dot{\chi}_L(0)}{\chi_L(0)}, \quad (4.3a)$$

with Δ_L and $\bar{\Delta}_L$ from Eqs. (2.13), incorporate the choice of vacuum state for the field, just as do the coefficients $\kappa_L^{(\pm)}$ of Eq. (2.6a). For the Euclidean or Chernikov-Tagiurov vacuum choice used here, their values are

$$\gamma_L = 2 \left| \frac{\Gamma\left(\frac{\frac{3}{2} + \lambda_1 + iqa}{2}\right)}{\Gamma\left(\frac{\frac{1}{2} + \lambda_1 - iqa}{2}\right)} \right|^2. \quad (4.3b)$$

This specification is equivalent to the coefficient choice (2.20).

All the particle properties of interest can be calculated once the expansion coefficients ξ_L for the wave packet Φ are known. With the γ_L real, condition (4.1b) implies

$\xi_L = \xi_L^*$. Expansion (3.2) and form (4.2) then yield the general form

$$\xi_L = a^{(N-1)/2} \left(\frac{\gamma_L}{2}\right)^{1/2} \int \Phi(0, \Omega_N) \mathcal{Y}_L(\Omega_N) d\Omega_N. \quad (4.4a)$$

The calculations displayed here are for the case of three spatial dimensions ($N = 3$), and a value for parameter (2.6b) of $qa = \frac{1}{2}$. The spherical symmetry of the wave packet implies that only $\ell_2 = \ell_3 = 0$ harmonics contribute. The relevant coefficients are thus

$$\begin{aligned} \xi_{\ell_1 00} &= 4\pi a \left(\frac{\gamma_{\ell_1}}{2}\right)^{1/2} \frac{K}{(2\pi\sigma^2)^{1/2}} \\ &\quad \times \int_0^\pi \mathcal{Y}_{\ell_1 00}(\theta_1) \exp\left(-\frac{\theta_1^2}{2\sigma^2}\right) \sin^2 \theta_1 d\theta_1 \\ &= \frac{2aK}{\sigma} (\pi\gamma_{\ell_1})^{1/2} \\ &\quad \times \int_0^\pi \frac{1}{(2\pi^2)^{1/2}} \frac{\sin(\lambda_1 \theta_1)}{\sin \theta_1} \exp\left(-\frac{\theta_1^2}{2\sigma^2}\right) \sin^2 \theta_1 d\theta_1 \\ &\simeq \frac{aK\gamma_{\ell_1}^{1/2}}{2} \left(e^{-\ell_1^2 \sigma^2/2} - e^{-(\ell_1+2)^2 \sigma^2/2}\right). \end{aligned} \quad (4.4b)$$

The approximation in the last expression is that of extending the integration from π to infinity; for σ values substantially less than unity the error introduced is negligible. It is even possible to calculate the coefficients $\xi_{\ell_1 00}$ for the $\sigma \rightarrow 0$ limit of this wave packet, i.e., a genuinely pointlike δ -function packet at $t = 0$. This yields

$$\xi_{\ell_1 00}^{(\delta)} = \frac{aK}{2\pi} \gamma_{\ell_1}^{1/2} (\ell_1 + 1), \quad (4.4c)$$

where again K is determined numerically by imposing condition (3.5) on the coefficients. In this case, since the expansion for Φ is formally divergent, care must be taken to discard numerical artifacts associated with the cutoff in the sum over ℓ_1 values. Here the convergent series for finite σ values are taken to 50 terms; the series for the $\sigma \rightarrow 0$ limit are cut off at 100 terms.

The classical evolution of the wave packet, and the associated quantum energies and detector responses described in the previous section, are obtained via numerical evaluation of the necessary gamma and hypergeometric functions. As both of these can involve sums of large terms with alternating signs, roundoff errors are a significant concern. The results shown here were calculated in quadruple-precision—128-bit real and 256-bit complex—arithmetic to suppress these errors. The sums over ℓ_1 were taken over 50 terms for the (convergent) finite- σ cases, and over 100 terms for the $\sigma \rightarrow 0$ limit case.

The classical evolution of the Gaussian wave packet is shown in Fig. 1. The field Φ is shown rescaled by a factor $\cosh^{3/2}(t/a)$, to compensate for the diminution of Φ associated with the increasing physical volume of the space. Over the time interval shown, the radius of the space increases by a factor of over 1.6×10^6 , the volume by over 4.3×10^{18} . The initially localized packet spreads

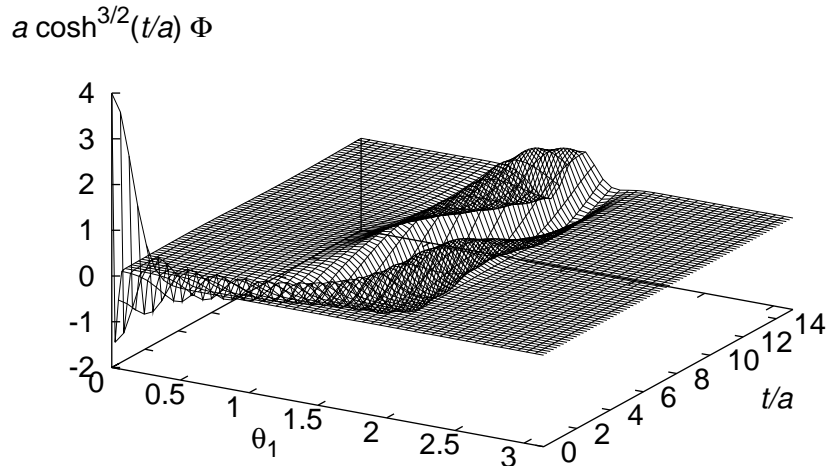


FIG. 1: Evolution of a spherically symmetric, initially Gaussian scalar wave packet in de Sitter space, centered on the “north pole” ($\theta_1 = 0$). The (angular) width of the initial Gaussian here is $\sigma \doteq 0.1414$. The field Φ is rescaled by $\cosh^{3/2}(t/a)$ to compensate for the physical expansion of the space.

quickly to the two-dimensional “equator” of the space, i.e., the sphere $\theta_1 = \pi/2$. This general behavior is quite insensitive to the initial width σ of the packet.

The excitation energies (3.17) of coherent quantum field states corresponding to such classical wave packets, above the Euclidean vacuum, are shown in Fig. 2. For the initially static wave packets used here, the energies are time-symmetric. As it happens, the excitation energies (3.6) of smeared one-particle states for the same wave packets are indistinguishable from these on the scale of this graph. The most striking features of these energies are that the oscillations apparent in the individual normal-mode energies persist, and the amplitudes of these oscillations—though not their phases—are insensitive to the initial width of the classical wave packet. Moreover, for the parameters used here, the mass of the field is $\mu = 1.581 a^{-1}$; the oscillating energies are always substantially above that value. This contrasts with the energy of a *classical* particle, which would rapidly redshift to the value μ . The periods of the oscillations all approach $6.28 a$, the same as that of the individual-mode energy oscillations (2.17a) for the value of q taken here.

The detector response functions, above the vacuum contribution, for smeared one-particle and coherent field states corresponding to these wave packets are shown in Figs. 3–5. Because the wave packets are localized, the response depends strongly on the location of the detector. Responses for coherent states, with the detector comoving—i.e., sitting—at the “north pole” of the space ($\theta_1 = 0$, the center of the wave packet) are shown

in Fig. 3. Response functions for smeared one-particle states corresponding to the same wave packets are indistinguishable from these at this position. However, for a detector comoving anywhere on the “equator” ($\theta_1 = \pi/2$), the responses for the two field states are distinguishable at low energies, although the response functions (probabilities) are some two orders of magnitude smaller. This is illustrated in Fig. 4 for a wave packet with $\sigma = 0.2236$; the results for other widths are similar in size, shape, and location. With the detector at the “south pole” ($\theta_1 = \pi$), the responses for smeared one-particle states are two orders of magnitude smaller still, as shown in Fig. 5. The responses for coherent states for the same wave packets are at least three orders of magnitude smaller even than these at this position; in fact they are below the precision of these calculations. In all cases the response functions retain the finite peak height and width which characterize the individual normal-mode excitations. Of course here both the irreducible, individual-mode widths and the superposition of modes required to form the wave packets contribute to the observed peak widths. The peak energies increase monotonically with increasing localization of the wave packet (decreasing σ), as might be expected, for the north-pole detector (Fig. 3). Notably, however, this progression is not apparent at the other detector positions. There the peak *heights* decrease monotonically with decreasing σ , i.e., the more strongly localized particles are simply less detectable at these locations.

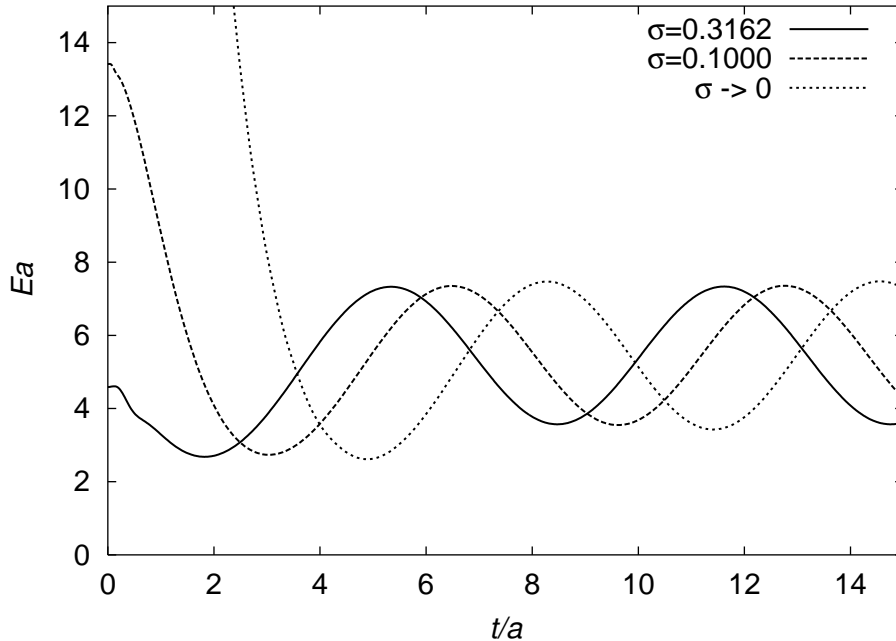


FIG. 2: Excitation energies \mathcal{E}_c of coherent (Glauber) field states corresponding to initially-Gaussian classical wave packets. The energy for the initially pointlike ($\sigma \rightarrow 0$) wave packet decreases monotonically from a value of $80.4133 a^{-1}$ at $t = 0$ to the region shown here.

V. CONCLUSIONS

Localized first-quantized or classical particles are readily described in a quantized linear field theory on a curved-spacetime background. Smearing one-particle field states and coherent field states provide straightforward means for this. Dynamical features of the particles, such as energy expectation values and detector response functions in these states, are easily evaluated. For particles in hyperbolically (exponentially) expanding de Sitter space, the distinctive behavior of these features for normal-mode excitations of the field persists for at least some localized-particle states: Energy expectation values oscillate, and detector response functions are finite, with finite width in energy. While states describing more realistic particles, e.g., those localized at arbitrary positions at arbitrary times, would require more complicated normal-mode expansions than those used here, it is to be expected that these behaviors would still characterize the particles.

The smeared one-particle state construction is more commonly associated with a single particle in quantum field theory, although coherent field states might be more apt descriptions of a particle with a well-defined (first-quantized) wave function, or of a classical field wave packet. For the simple wave packets examined here, the energy expectation values of the states do not distinguish between the two descriptions, but the detector response functions—especially, for detectors located away from the initial localization of the wave packets—could do so.

The interpretation of these features in terms of physical measurements is, however, somewhat subtle. For example, if the scale factor a in de Sitter metric (2.1) is taken to be c/H_0 , with c the speed of light and $H_0 = 75 \text{ km/s/Mpc}$, then its value in ordinary units is $a \doteq 1.2 \times 10^{26} \text{ m}$. The field mass μ corresponding to the examples of Sec. IV above (with $qa = \frac{1}{2}$) is $\mu \doteq 1.58\hbar c/a \doteq 2.5 \times 10^{-33} \text{ eV}$. This is of the same order of magnitude as the ultralow mass proposed by Parker and Raval [6, 7]. But in that case the period of the energy oscillations of Fig. 2 is $2\pi a/c \doteq 13 \text{ Gyr}$ —nearly the presently accepted age of the Universe. Larger q and μ values yield faster oscillations but much smaller amplitudes. And for the energy oscillations to be detectable, \mathcal{E} must be measurable to a precision substantially smaller than the oscillation amplitude in a time smaller than, say, one radian of the oscillation. With the values used here the late-time amplitudes are all about $2 a^{-1}$, while the time for one radian of oscillation is a (in geometrized units once again), so energy-time uncertainty allows detection, but with little leeway. Of course these energies are not energy eigenvalues but expectation values, so measurements of large numbers of identical particles may allow greater precision. Moreover, as the energy-time uncertainty relation arises not from fundamental commutation relations but from analysis of the measurement interaction, a more detailed examination of the energy-measurement process might be needed to clarify this issue. In this respect the detector responses in Figs. 3–5 could be considered prototypical

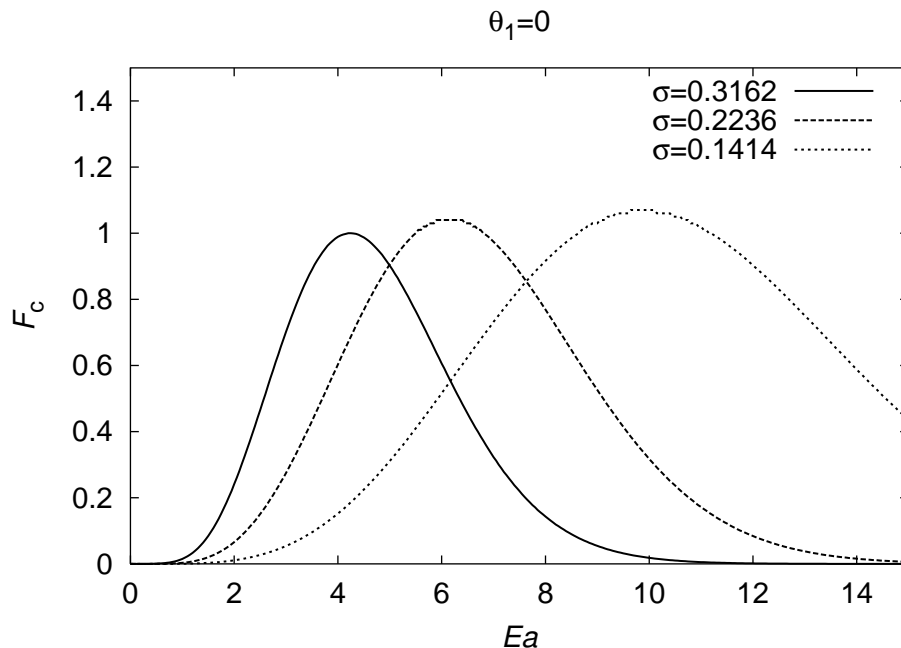


FIG. 3: Detector response functions \mathcal{F}_c for coherent field states corresponding to initially-Gaussian wave packets, above the Euclidean-vacuum contribution (“dark current”). The detector is comoving at the “north pole” $\theta_1 = 0$. Responses for smeared one-particle states corresponding to the same wave packets are indistinguishable from these on this scale.

particle-energy measurements. These are integrals over all time, so they reveal no time dependence. (Switching the detectors on and off introduces extraneous excitations, difficult to disentangle from interactions with the field φ .) And the energy dependence of the responses is sensitive to detector location. In these calculations the detector is taken to be a pointlike quantum system unaffected by the spacetime geometry—hence the ordinary Fourier transforms in Eq. (2.18). A future analysis of the interaction of two genuinely de Sitter-space quantum systems may shed more light on the prospects for observing such quantum/spacetime-dynamical phenomena.

Acknowledgments

Portions of this work were supported by the U. S. National Science Foundation under Grants No. PHY89–22140 at Washington University in St. Louis and No. PHY91–05935 at the University of Wisconsin–Milwaukee. I thank Professor Robert Pasken of the Department of Earth and Atmospheric Sciences, Saint Louis University, for invaluable assistance with the numerical calculations of Sec. IV.

-
- [1] S. W. Hawking, *Nature (London)* **248**, 30 (1974).
 - [2] A. H. Guth, *Physical Review D* **23**, 347 (1981).
 - [3] I. H. Redmount, *Physical Review D* **40**, 3343 (1989).
 - [4] G. Daues and I. H. Redmount, *Physical Review D* **47**, 2423 (1993).
 - [5] S. Perlmutter et al., *Nature (London)* **391**, 51 (1998).
 - [6] L. Parker and A. Raval, *Physical Review D* **60**, 063512 (1999).
 - [7] L. Parker and A. Raval, *Physical Review D* **60**, 123502 (1999).
 - [8] L. M. Burko, A. I. Harte, and E. Poisson, *Physical Review D* **65**, 124006 (2002).
 - [9] C. W. Misner, K. S. Thorne, and J. A. Wheeler, *Gravitation* (W. H. Freeman, San Francisco, 1973).
 - [10] P. M. Garnavich et al., *Astrophysical Journal* **493**, L53 (1998).
 - [11] M. Gutzwiller, *Helvetica Physica Acta* **29**, 313 (1956).
 - [12] K. Freese, C. T. Hill, and M. Mueller, *Nuclear Physics B* **255**, 693 (1985).
 - [13] B. Ratra, *Physical Review D* **31**, 1931 (1985).
 - [14] J. S. Dowker and R. Critchley, *Physical Review D* **13**, 3224 (1976).
 - [15] T. S. Bunch and P. C. W. Davies, *Proceeding of the Royal Society of London A* **360**, 117 (1978).
 - [16] N. D. Birrell and P. C. W. Davies, *Quantum Fields in Curved Space* (Cambridge University Press, Cambridge, England, 1982).
 - [17] W. G. Unruh, *Physical Review D* **14**, 870 (1976).
 - [18] B. S. DeWitt, in *General Relativity: An Einstein Centenary Survey*, edited by S. W. Hawking and W. Israel (Cambridge University Press, Cambridge, England, 1979), pp. 690–695.

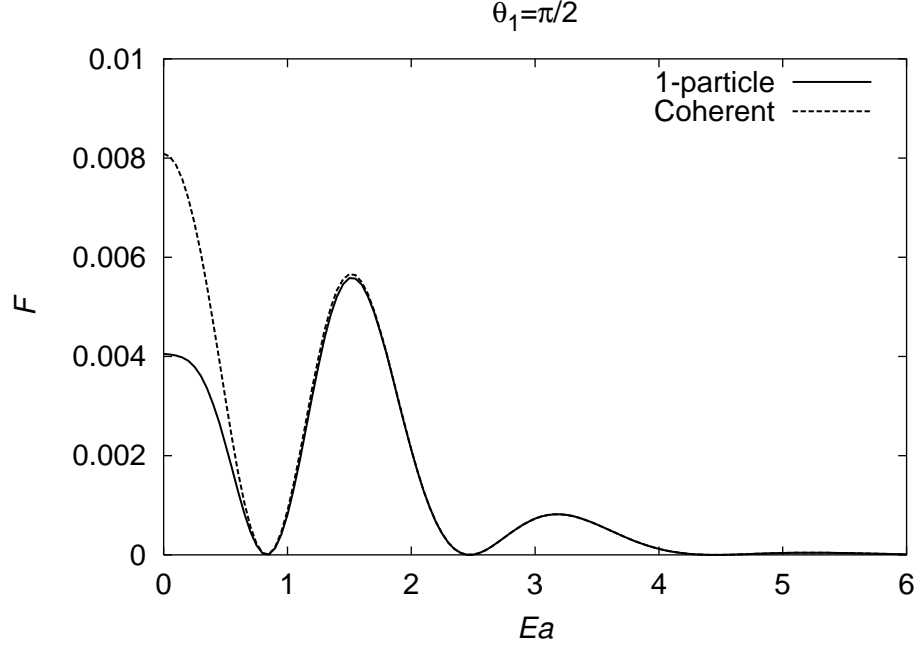


FIG. 4: Detector response functions \mathcal{F}_1 and \mathcal{F}_c for smeared one-particle and coherent states corresponding to an initially-Gaussian wave packet with $\sigma = 0.2236$. Here the detector is comoving at the “equator” ($\theta_1 = \pi/2$).

[19] C. J. C. Burges, Nuclear Physics B **247**, 533 (1984).

[20] G. W. Gibbons and S. W. Hawking, Physical Review D **15**, 2738 (1977).

[21] N. A. Chernikov and E. A. Tagirov, Annales de l’Institut Henri Poincaré **9A**, 109 (1968).

[22] E. Schrödinger, Naturwissenschaften **14**, 664 (1926).

[23] B. L. Schumaker, Physics Reports **135**, 317 (1986).

[24] W.-M. Zhang, D. H. Feng, and R. Gilmore, Reviews of Modern Physics **62**, 867 (1990).

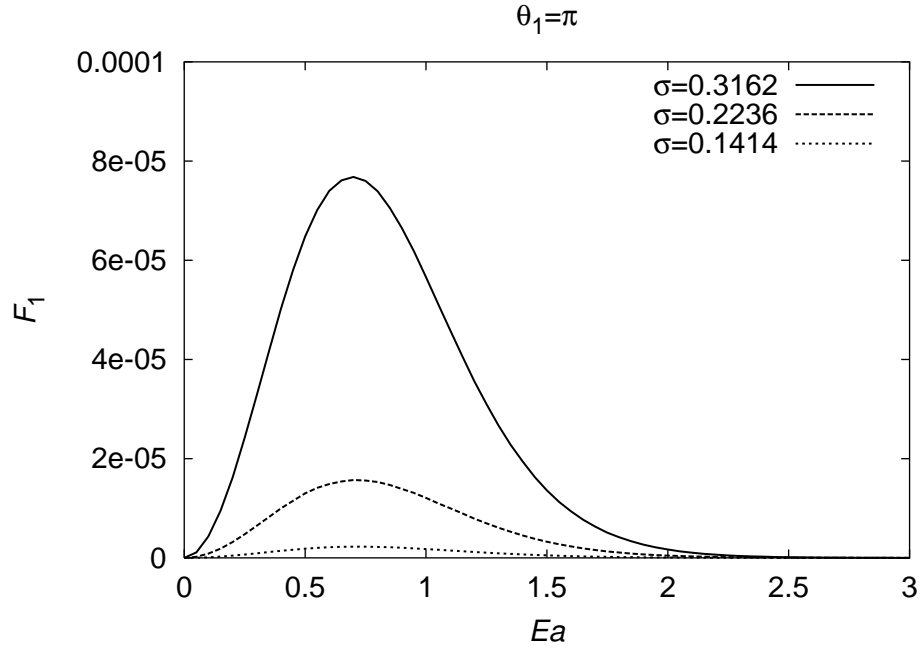


FIG. 5: Detector responses \mathcal{F}_1 for smeared one-particle states corresponding to initially-Gaussian wave packets. Here the detector is comoving at the “south pole” ($\theta_1 = \pi$). Responses for coherent states for the same wave packets, for this detector position, are negligible on the scale of this graph (and below the resolution of the calculation).